

# A 35- $\mu\text{m}$ Pitch IR Thermo-Mechanical MEMS Sensor With AC-Coupled Optical Readout

Ulas Adiyen, Fehmi Çivitçi, Onur Ferhanoglu, Hamdi Torun, *Member, IEEE*, and Hakan Urey, *Senior Member, IEEE*

**Abstract**—A thermo-mechanical MEMS detector with 35- $\mu\text{m}$  pixel pitch is designed, fabricated, and characterized. This fabricated design has one of the smallest pixel sizes among the IR thermo-mechanical MEMS sensors in the literature. The working principle of the MEMS detector is based on the bimaterial effect that creates a deflection when exposed to IR radiation in the 8–12- $\mu\text{m}$  waveband. The nanometer level out of plane mechanical motion is observed in response to IR heating of the pixel, which is detected by a diffraction grating-based optical readout. Performance of MEMS sensor arrays with optical readout have been limited by a large DC bias that accompanies a small AC signal. We developed a novel optical setup to reduce the DC term and the related noise using an AC-coupled detection scheme. Detailed noise characterization of the pixel and the readout system is reported in this paper. The noise equivalent temperature difference of our detector is measured as 216 mK using  $f/0.86$  lens with the AC-coupled optical readout. Finally, we obtained a thermal image using a single MEMS pixel combined with a scanning configuration. Despite the reduced pixel size, the measured noise levels are comparable to the state-of-the-art thermo-mechanical IR sensors.

**Index Terms**—Thermo-mechanical MEMS, IR imaging, optical readout, diffraction grating.

## I. INTRODUCTION

INFRARED (IR) imaging in the 8–12  $\mu\text{m}$  spectral region (long wave IR) is of great importance to a wide range of applications such as night vision, environmental monitoring, astronomy and biomedical applications. These applications not only require having low noise equivalent temperature difference (NETD) (less than 250 mK)—high sensitive systems—but also low cost, low power consuming and light weight systems. Uncooled IR imaging systems can meet the requirements offering high performance, low cost, lightweight compact packages [1], [2]. Microbolometers are the most used focal plane array (FPA) technology among the uncooled IR detectors [3]. Despite their high performance in IR imaging, the system and fabrication complexity, as well as its cost make thermo-mechanical detectors a cost-effective, and promising alternative technology

[3]–[8]. The principle of thermo-mechanical detectors is based on the bending of the bimaterial cantilevers due to absorbed IR radiation. This mechanical motion can be detected via optical or electrical methods. Optical readout methods play a critical role in IR imaging, allowing passive, electric connection free, sensor architecture that results in high thermal insulation and thus high temperature sensitivity. Owing to their passive nature, these thermo-mechanical sensor arrays can be easily scaled up to larger formats. In this manuscript, for the first time we present a 35- $\mu\text{m}$  pixel pitch thermo-mechanical MEMS detector with a novel mechanical design that allows piston-like motion, utilizing diffraction grating based interferometric AC coupled optical readout.

The pixel pitch of the presented detector in this paper is one of the smallest among the other fabricated MEMS based IR thermo-mechanical detectors [9]. Decreasing the size of pixel pitch for the mature bolometer technology is a major research field to make them smaller, cheaper, lighter and less power consuming [3]. For instance, there are bolometer FPAs having 17 and 25  $\mu\text{m}$  pixel pitches fabricated as different formatted arrays and the tendency is toward further decreasing the pixel pitch [10]. However for the emerging technology of thermo-mechanical MEMS detectors, there has been no significant attempt to reduce the pixel pitch which are generally greater than or equal to 50  $\mu\text{m}$  [4]–[7]. There have been a few studies on reducing the size in IR thermo-mechanical detectors. One of them has yielded a decrease of pixel pitch down to 42  $\mu\text{m}$  [11], while some other studies theoretically investigated the feasibility of 25  $\mu\text{m}$  pixel pitch [8], [12]. A thermo-mechanical detector with a pitch size of 20  $\mu\text{m}$  was demonstrated in ref. [9]. The readout setup uses quad-cells readout for single elements and a CCD readout for array structures. On the other hand, we implement a diffraction grating based interferometer for the readout that offers high sensitivity at the expense of the need for placing a diffraction grating under the pixel which can be a limiting factor to reduce the size.

Although small pixel pitch offers fabrication of large formatted arrays, there are challenges associated with decreasing the pixel pitch such as low fill factor, lower thermal isolation and reduced responsivity due to shorter bimaterial legs. In order to increase the responsivity, detailed analyses are needed for the length and thickness optimization of the bimaterial pair. SiNx (nitride) is a suitable absorber material in the far IR band [4]–[8] and is commonly used as the structural material. In combination with nitride, aluminum (Al) forms a strong thermal mismatch pair with its high thermal expansion coefficient [6].

The pitch size of the pixel shown in Fig. 1(a) is 35  $\mu\text{m}$ . The pixel is made of 150-nm-thick Al and 150-nm-thick nitride

Manuscript received October 1, 2014; revised November 28, 2014; accepted December 15, 2014. This work was supported by Aselsan Inc., Turkey.

U. Adiyen, F. Çivitçi, and H. Urey are with the Electrical and Electronics Engineering Department, Koç University, 34450 İstanbul, Turkey (e-mail: uladiyan@ku.edu.tr; fcivitci@ku.edu.tr; hurey@ku.edu.tr).

O. Ferhanoglu is with the Electronics and Communication Engineering Department, Istanbul Technical University, 34469 Istanbul, Turkey (e-mail: ferhanoglu@itu.edu.tr).

H. Torun is with the Electrical and Electronics Engineering Department, Boğaziçi University, 34342 Istanbul, Turkey (e-mail: hamdi.torun@boun.edu.tr).

Color versions of one or more of the figures in this paper are available online at <http://ieeexplore.ieee.org>.

Digital Object Identifier 10.1109/JSTQE.2014.2384503

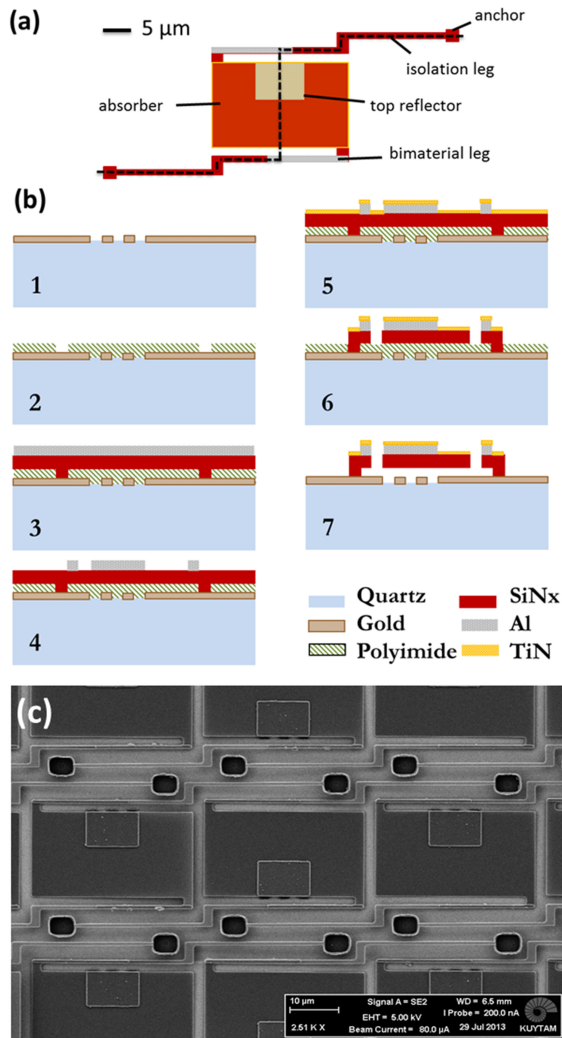


Fig. 1. (a) Single MEMS pixel geometry (top view) (b) Fabrication steps: (1) Patterning of gold grating (2) Polyimide spinning and definition of anchors (3) SiNx and Al deposition (4) Al patterning (5) TiN deposition (6) TiN and SiNx patterning (7) Release (c) SEM image of a part of the FPA.

that form bimaterial legs with a length of  $20 \mu\text{m}$ . The isolation leg is  $42 \mu\text{m}$  long excluding the joints and the anchor. The isolation legs are longer as compared to the bimaterial legs to minimize thermal conductance for better performance. Fig. 1(b) illustrates the fabrication steps. First, a gold layer is evaporated and patterned as a diffraction grating onto a quartz substrate using a lift-off process. Then, a polyimide layer is deposited as a sacrificial layer and patterned. After that, the structural nitride and Al layers are deposited and then Al is patterned to form the top reflector and bimaterial legs. A thin layer of Titanium Nitride (TiN) is further deposited on top of the structural nitride layer to enhance IR absorption. Then nitride and TiN is patterned using the same mask and the structure is released using oxygen plasma etching. Fig. 1(c) shows a part of the FPA in the scanning electron microscope (SEM) image. The reflectors on top of the pixel bodies are placed hexagonally in the array to mitigate the optical cross talk during array readout [13].

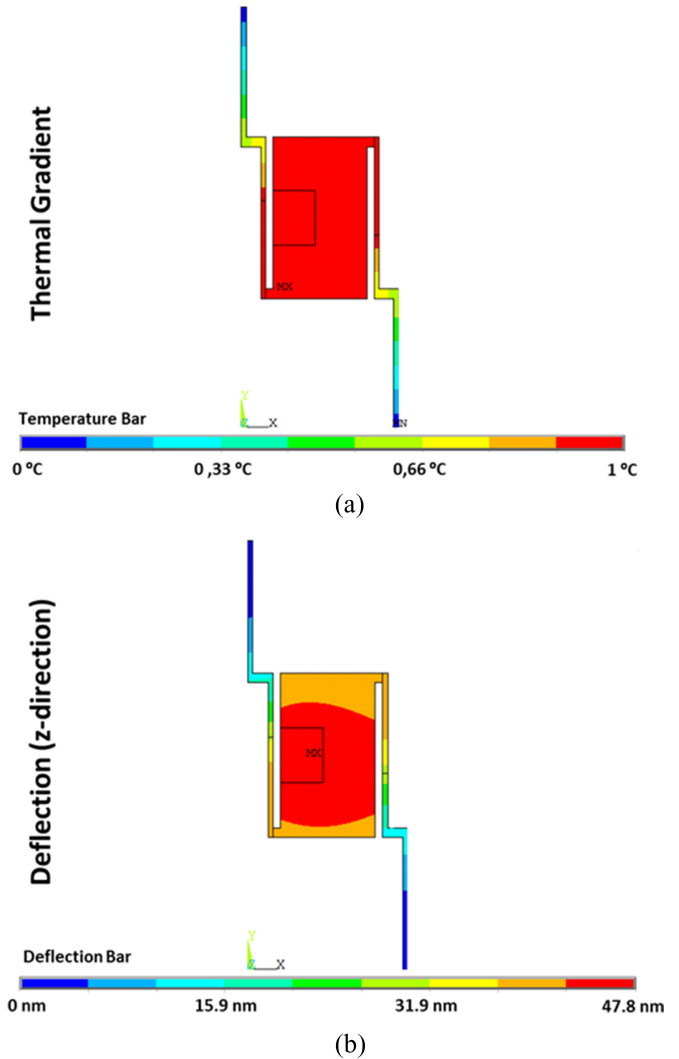


Fig. 2. (a) Thermal gradient of the MEMS pixel when  $1 \text{ }^\circ\text{C}$  is applied to the absorber (Anchors are  $0 \text{ }^\circ\text{C}$ ). (b) Mechanical deflection analysis for  $1 \text{ }^\circ\text{C}$  change in the pixel using FEM.

Fig. 2 shows the temperature distribution and the resulting thermo-mechanical deflection of a pixel based on finite element methods (FEM) analysis. A thermal gradient along the pixel is observed when a temperature load of  $1 \text{ }^\circ\text{C}$  is applied on the absorber, as illustrated in Fig. 2(a). This results in an out-of-plane deflection of  $47.8 \text{ nm}$ , as illustrated in Fig. 2(b).

Our unique mechanical design, capable of out-of-plane, piston-like movement, is compatible with our grating interferometer based optical readout, owing to the crosswise configuration of the legs. The out-of-plane motion is ensured through the two-end-fixed design that is composed of two legs, each having two joints. Furthermore, the design is immune to environmental vibrations due to its high mechanical resonant frequency of  $\sim 18 \text{ kHz}$ , according to FEM analysis.

## II. OPERATION PRINCIPLE

The diffraction grating interferometer based readout method has been previously employed in thermal detectors [4], [6]. Typically the  $\pm 1$ st diffraction order is used to monitor the sub-micron

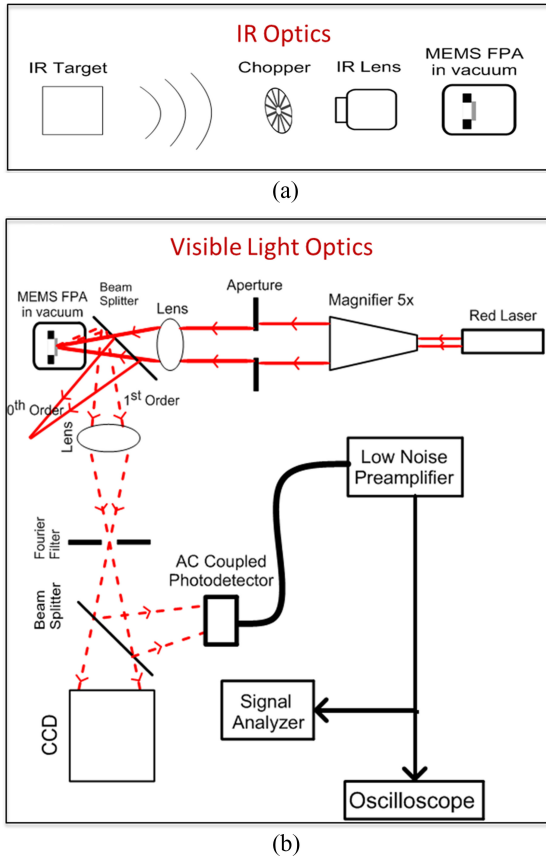


Fig. 3. Experimental setup of single pixel optical readout: (a) IR optics part, (b) Visible light optics part.

mechanical displacement with sub-nanometer precision [4], [6]. The limiting performance factor for the thermo-mechanical detector is the optical readout noise that arises from the CCD sensor array and the laser. In addition, bias on the diffracted light [4]–[11] limits the dynamic range and increases the shot noise.

Since CCD noise poses a significant limit, characterization for the performance of the MEMS device alone is hampered. In order to isolate the optical noise from the performance of the MEMS sensor, we propose an AC coupled optical readout setup, as illustrated in Fig. 3. Accordingly, the IR target is modulated using a rotating chopper. The modulated IR radiation is focused on the MEMS device using an IR lens, with a focal length of 50 mm (see Fig. 3(a)). The visible optics part of the experimental setup is given in Fig. 3(b). First, the illumination system focuses the laser light onto a single MEMS pixel. We use an ultra-low noise red laser preceding a  $5\times$  magnifier. After beam-shaping with a circular aperture, we focus the laser on an individual array element using a 100 mm focal length lens. We then image the first diffraction orders reflected back from the MEMS device on the CCD with a single lens and an aperture at the Fourier plane, while also monitoring the intensity of the first order with a photodetector (PD). This PD, which is connected to a wide band-pass filter having a center frequency of 10 Hz, rejects the DC component of the diffracted light. We fine tune the focusing until a single diffracted spot appears at the CCD screen. After

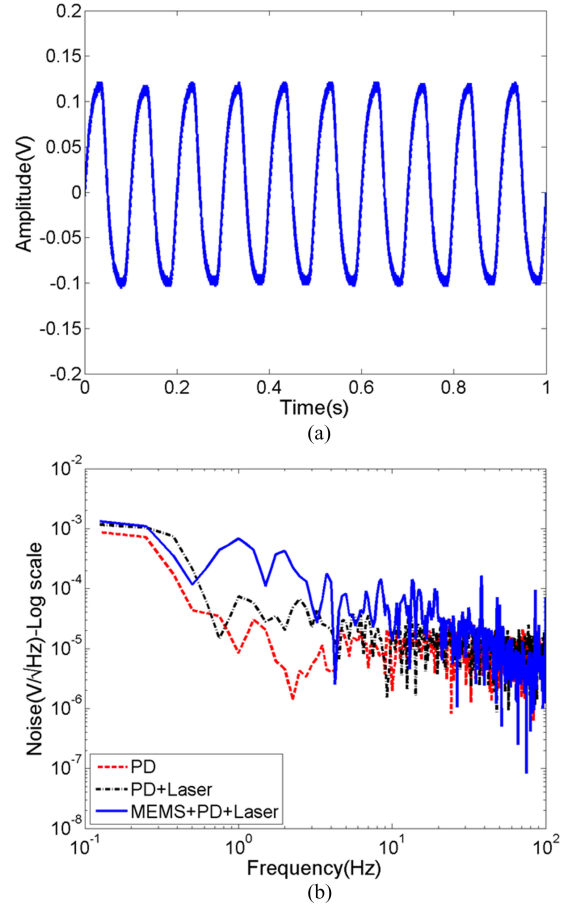


Fig. 4. (a) 10 Hz AC signal for 50 °C temperature difference. (b) Noise levels of the optical readout system with the contribution of the PD, laser and MEMS device.

tight focusing onto a single element, we gather the relevant intensity data from the PD in response to the chopped IR target.

Since the MEMS FPAs are tailored for real time imaging applications, the system is designed to work with a 30 fps CCD camera. Therefore a low noise preamplifier is utilized just after the PD, implementing a unity gain low pass filter with a 30 Hz cutoff frequency. An oscilloscope and a signal analyzer are connected to the low noise preamplifier. The oscilloscope is used in measuring the signal level when the MEMS device is exposed to a chopped blackbody source. Second, while the IR target is blocked, the noise measurement of the system is held using both the oscilloscope and the signal analyzer to mutually cover the entire frequency range of 0–30 Hz. A Thermoelectric cooler (TEC) module is used as an IR target that is placed before a rotating chopper to carry out the AC coupled readout.

### III. EXPERIMENTAL RESULTS

In the experiments, the TEC module was heated up to 75 °C where the background temperature was 25 °C. The response of the selected MEMS pixel to the TEC module, which was chopped at 10 Hz, is given in Fig. 4(a). The peak-to-peak signal level ( $V_s$ ) was 220 mV for the temperature difference of  $\Delta T = 50$  °C. We also deduced the thermal time constant as 15 ms based

TABLE I  
EXPERIMENTALLY DETERMINED NETD VALUES

Noise Sources	NETD [mK]
NETD <sub>TOTAL</sub> (MEMS Total Noise)	216
NETD <sub>OPT</sub> (Optical Readout Noise)	166
NETD <sub>MEMS</sub> (MEMS Noise)	140

on the signal, which is an important figure of merit to understand the capability of the system for 30-fps real time applications.

The noise measurement was performed in three steps, through isolating one noise component at a time. First, we blocked the laser and measured the noise of the PD. Second we checked the contribution of the laser intensity noise, while the MEMS was by-passed with a switch mirror. Then, the intensity of the beam collected at the PD was adjusted to that of the first diffracted order using neutral density filters. Finally, we measured the entire system noise including the MEMS device, which will be used in the calculation of the NETD.

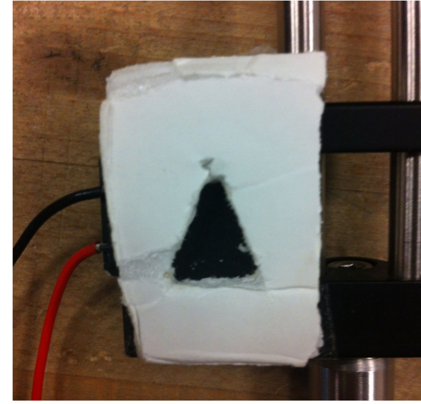
Fig. 4(b) depicts the noise levels of the PD, laser and MEMS. When the laser is turned ON, the noise increases particularly for the lower frequencies ( $< 10$  Hz), due to a combination of laser intensity noise and low frequency vibrations associated with our setup. The total noise is further above both PD and laser noise sources, as expected, due to contribution from the MEMS noise sources. Thermo-mechanical, background fluctuation and temperature fluctuation noises are among MEMS related noise sources, which are the fundamental limitations of the uncooled thermo-mechanical IR detectors [14].

We integrated the total noise (MEMS + PD + Laser) between 0–30 Hz for extracting SNR and NETD of the system. We wanted to limit the noise spectrum to 0–30 Hz as an ideal case to characterize the system as if we can capture 15 Hz video content for real time video applications. The SNR calculation is given in Eq. (1) where  $V_s$  is the peak to peak signal level and *Noise* refers to the total noise measured for the system, as illustrated in Fig. 4(b). The noise power was then integrated, where the lower bound ( $f_1$ ) was taken as 0 and the upper bound ( $f_2$ ) as 30 Hz. Once SNR is determined, NETD can be calculated by taking the ratio of  $\Delta T=50$  °C to the SNR by using Eq. (2). The NETD of the selected pixel, whose signal and noise levels are given in Fig. 4, was calculated as 216 mK

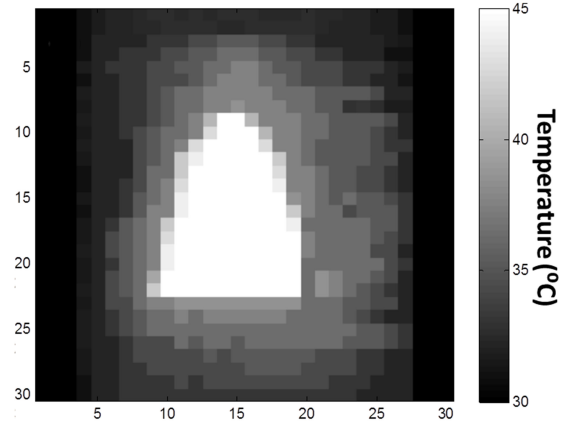
$$\text{SNR} = V_s / \sqrt{\int_{f_1}^{f_2} \text{Noise}^2} \quad (1)$$

$$\text{NETD} = \Delta T / \text{SNR}. \quad (2)$$

As an alternative way, we calculate the NETD according to the output given in Fig. 4(a) without limiting the noise spectrum to 0–30 Hz while calculating the total noise. In this case the signal level is the mean of the peak to peak signal amplitude for different cycles at 10 Hz in Fig. 4(a). Similarly, the noise is the standard deviation of the peak to peak signal amplitudes for different cycles as different measurements. We calculated



(a)



(b)

Fig. 5. (a) Visible image of the target. (b) Thermal image of the target.

NETD as 303 mK using this approach that sets an upper bound for the noise performance.

NETD calculation procedure is also applied to PD + Laser (optical) noise data (see Fig. 4(b)) to determine the contribution of optical readout noise. Then noise sources associated with MEMS and optical readout are extracted using:

$$\text{NETD}_{\text{TOTAL}} = \sqrt{\text{NETD}_{\text{OPT}}^2 + \text{NETD}_{\text{MEMS}}^2}. \quad (3)$$

The NETD<sub>OPT</sub> is calculated as 166 mK whereas the NETD<sub>MEMS</sub> is found as 140 mK, as illustrated in Table I. Using a low-noise laser and PD will allow for approaching to the measured NETD limit of 140 mK, which is associated with MEMS, for our system. Additionally, theoretical calculations lead to an NETD level of 35 mK for the MEMS sensor [13], assuming thermo-mechanical sensitivity of 47.8 nm/K based on finite element simulations, 0.43 fill factor, 30 Hz detection bandwidth, and 0.86 f#, calculated thermal conductance of  $12 \times 10^{-8}$  W/K and 80% IR transmittance.

The discrepancy between theoretical and experimental NETD values associated with MEMS is attributed to the imperfections in the fabrication process possibly resulting in an increase for thermal conductance and a decrease in thermo-mechanical deflection. Furthermore, low frequency vibrations in our setup due

to the vacuum pump also appear within 0–30 Hz bandwidth of the MEMS noise spectrum.

In addition, thermal imaging was performed by using the selected pixel. A triangular mask, covering a TEC module is used as an IR target (see Fig. 5(a)). The temperature of the TEC was adjusted as  $\Delta T = 15^\circ\text{C}$  above room temperature. The TEC was placed before the chopper and mounted on an XY stage to scan the whole target with 100  $\mu\text{m}$  step size at 30 steps in both  $x$  and  $y$  directions. The target was placed 500 mm in front of the IR lens, providing a demagnification of  $\sim 10\times$  on the array. The response of the single pixel readout was recorded as a peak to peak voltage value. Then the data was processed and registered as a thermal image as shown in Fig. 5(b). The temperature levels lie between 30–45  $^\circ\text{C}$  for the lowest and highest observed temperatures respectively.

The AC coupled optical readout method is favorable for single element operation, but for the array structures a custom CMOS read-out integrated circuit (ROIC) can be used. Such ROIC circuitry [13] includes photodiodes, trans-impedance amplifiers, bandwidth limiting and DC eliminating filters, together with analog multiplexers and decoders for pixel selection.

#### IV. CONCLUSION

Design, fabrication and IR characterization of a 35  $\mu\text{m}$  pixel pitch thermo-mechanical MEMS detector is presented for the first time. A unique mechanical design employing piston-like out-of-plane motion has been proposed that is compatible with a diffraction grating based optical readout. Our low-noise, single pixel AC coupled optical readout significantly isolates the noise associated with the MEMS pixel only. The NETD of the selected MEMS pixel is measured as 216 mK, with which we acquire a thermal image through scanning the target. Despite 35  $\mu\text{m}$  pixel pitch, the measured NETD is comparable to the state-of-the-art thermo-mechanical IR sensors that are larger in size [15], [16]. We calculated the theoretical NETD for the MEMS as 35 mK without the optical readout noise which implies that the fundamental limit for NETD is below 50 mK using this pixel design with the further development of the implemented method. We envision improvement in spatial and temperature resolution of thermo-mechanical MEMS detectors using this method.

#### ACKNOWLEDGMENT

The authors would like to thank Prof. T. Akın and O. Akar from Middle East Technical University Microelectronics Center: METU-MET for fabrication of the arrays.

#### REFERENCES

- [1] A. Rogalski, "History of infrared detectors," *Opto-Electron. Rev.*, vol. 20, no. 3, pp. 279–308, Sep. 2012.
- [2] A. Rogalski, "Infrared detectors: An overview," *Infrared Phys. Technol.*, vol. 43, nos. 3–5, pp. 187–210, Jun. 2002.
- [3] M. Steffanson and I. W. Rangelow, "Microthermomechanical infrared sensors," *Opto-Electron. Rev.*, vol. 22, no. 1, pp. 1–15, Mar. 2014.
- [4] Y. Zhao *et al.*, "Optomechanical uncooled infrared imaging system: Design, microfabrication, and performance," *J. Microelectromech. Syst.*, vol. 11, no. 2, pp. 136–146, Apr. 2002.

- [5] D. Grbovic *et al.*, "Uncooled infrared imaging using bimaterial micro-cantilever arrays," *Appl. Phys. Lett.*, vol. 89, no. 7, p. 073118, 2006.
- [6] M. F. Toy, O. Ferhanoglu, H. Torun, and H. Urey, "Uncooled infrared thermo-mechanical detector array: Design, fabrication and testing," *Sens. Actuators A, Phys.*, vol. 156, no. 1, pp. 88–94, Nov. 2009.
- [7] S. Shi *et al.*, "Design, simulation and validation of a novel uncooled infrared focal plane array," *Sens. Actuators A, Phys.*, vol. 133, no. 1, pp. 64–71, Jan. 2007.
- [8] M. Steffanson *et al.*, "ARCH-type micro-cantilever FPA for uncooled IR detection," *Microelectron. Eng.*, vol. 98, pp. 614–618, Oct. 2012.
- [9] L. R. Senesac *et al.*, "IR imaging using uncooled microcantilever detectors," *Ultramicroscopy*, vol. 97, nos. 1–4, pp. 451–458, Oct. 2003.
- [10] F. Niklaus, C. Vieider, and H. Jakobsen, "MEMS-based uncooled infrared bolometer arrays: A review," *Proc. SPIE MEMS Technol. Appl.*, vol. 6836, p. 68360D, 2007.
- [11] Y. Ou *et al.*, "Design, fabrication, and characterization of a  $240 \times 240$  MEMS uncooled infrared focal plane array with 42- $\mu\text{m}$  pitch pixels," *J. Microelectromech. Syst.*, vol. 22, no. 2, pp. 452–461, Apr. 2013.
- [12] S. R. Hunter *et al.*, "High-sensitivity 25  $\mu\text{m}$  and 50  $\mu\text{m}$  pitch microcantilever IR imaging arrays," *Proc. SPIE, Infrared Technol. Appl.*, vol. 6542, pp. 65421F1–65421F13, May 2007.
- [13] R. B. Erarslan *et al.*, "Design and characterization of micromachined sensor array integrated with CMOS based optical readout," *Sens. Actuators A, Phys.*, vol. 215, pp. 44–50, Aug. 2014.
- [14] P. G. Datskos, N. V. Lavrik, and S. Rajic, "Performance of uncooled microcantilever thermal detectors," *Rev. Sci. Instrum.*, vol. 75, no. 4, pp. 1134–1148, 2004.
- [15] M. Erdtmann *et al.*, "Optical readout photomechanical imager: from design to implementation," *Proc. SPIE Infrared Technol. Appl.*, vol. 7298, pp. 72980I1–72980I8, May 2009.
- [16] B. Jiao *et al.*, "An optical readout method based uncooled infrared imaging system," *Int. J. Infrared Millimeter Waves*, vol. 29, no. 3, pp. 261–271, 2008.

**Ulas Adiyán** received the B.Sc. degree in telecommunication engineering and the M.Sc. degree in electronics and communication engineering both from Istanbul Technical University, Istanbul, Turkey, in 2007 and 2010, respectively. He is currently working toward the Ph.D. degree in the Electrical and Electronics Engineering Department at Koç University, Istanbul. He is currently a Member of OML Research Group where he is currently studying thermomechanical IR MEMS detectors. His research interests include development of microoptomechanical systems.

**Fehmi Çivitçi** received the M.Sc. degree in the Microelectromechanical Systems Group at the Middle East Technical University, Ankara, Turkey, and the Ph.D. degree in Integrated Optical Micro Systems Group at the University of Twente, Enschede, The Netherlands. He is currently working as a Postdoctoral Researcher in the Optical Microsystems Laboratory at Koc University, Istanbul, Turkey.

**Onur Ferhanoglu** received the B.S. and M.S. degrees from Bilkent University, Ankara, Turkey, in 2003 and 2005, respectively, in electrical engineering.

In 2005, he joined the Optical Microsystems Laboratory at Koç University as a Graduate Researcher, where he developed MEMS-based thermal imaging sensor arrays. During graduate studies, he visited The Johns Hopkins University in 2004, Georgia Tech. in 2007, and the École Polytechnique Fédérale de Lausanne in 2010, as a Research Scholar. After receiving the Ph.D. degree in 2011, he became a Postdoctoral Fellow at Femtosecond Laser Assisted Biophotonics Laboratory at the University of Texas at Austin, Austin, TX, USA, where he played a key role in the development of an ultrafast laser microsurgery scalpel from 2011 to 2014. He is currently appointed with the Electronics and Communications Engineering Department of Istanbul Technical University, Istanbul, Turkey. His research interests include biomedical optics and MEMS for medical applications.

**Hamdi Torun** (M'00) received the B.S. degree from Middle East Technical University, Ankara, Turkey, in 2003, the M.S. degree from Koç University, Istanbul, Turkey, in 2005, and the Ph.D. degree from the Georgia Institute of Technology, Atlanta, GA, USA, in 2009, all in electrical engineering. He was a Postdoctoral Fellow in the Department of Mechanical Engineering, Georgia Institute of Technology from 2009 to 2010. He is currently an Assistant Professor at the Department of Electrical and Electronics Engineering and affiliated with the Center for Life Sciences and Technologies at Boğaziçi University, Istanbul, Turkey.

His research interest includes development of microsystems for biomedical applications.

**Hakan Urey** (M'92–SM'09) received the B.S. degree in electrical engineering from Middle East Technical University, Ankara, Turkey, in 1992, and the M.S. and Ph.D. degrees in electrical engineering from the Georgia Institute of Technology, Atlanta, GA, USA, in 1996 and 1997, respectively.

After completing the Ph.D. degree, he joined Microvision, Inc., Seattle, WA, USA, as a Research Engineer, and he played a key role in the development of scanning display technologies. He was the Principal System Engineer when he left Microvision, Inc. in 2001 to join the College of Engineering, Koç University, Istanbul, Turkey, where he established the Optical Microsystems Laboratory. He is currently a Professor of electrical engineering at Koç University. He has published more than 50 journal and more than 100 conference papers, six edited books, and four book chapters, and he has about 30 issued and pending patents, which have been licensed to industry for commercialization. His research interests include microelectromechanical systems, microoptics, microoptoelectromechanical systems design, and laser-based 2-D/3-D display and imaging systems.

Dr. Urey is a Member of the SPIE, OSA, and the IEEE Photonics Society, and the Vice-President of the Turkey Chapter of the IEEE Photonics Society. He received the Werner von Siemens Faculty Excellence Award from Koç University in 2006, the Distinguished Young Scientist Award from the Turkish Academy of Sciences in 2007, the Encouragement Award from The Scientific and Technological Research Council of Turkey in 2009, the Outstanding Faculty of the Year Award from Koç University in 2013, and the European Research Council Advanced Investigator Grant in 2013.